

# ANALYZING LARGE AND SPARSE TENSOR DATA USING SPECTRAL LOW-RANK APPROXIMATION.

LARS ELDÉN\* AND MARYAM DEHGHAN†

June 22, 2022

**Abstract.** Information is extracted from large and sparse data sets organized as 3-mode tensors. Two methods are described, based on best rank-(2,2,2) and rank-(2,2,1) approximation of the tensor. The first method can be considered as a generalization of spectral graph partitioning to tensors, and it gives a reordering of the tensor that clusters the information. The second method gives an expansion of the tensor in sparse rank-(2,2,1) terms, where the terms correspond to graphs. The low-rank approximations are computed using an efficient Krylov-Schur type algorithm that avoids filling in the sparse data. The methods are applied to topic search in news text, a tensor representing conference author-terms-years, and network traffic logs.

**Key words.** tensor, multilinear rank, best rank-(p,q,r) approximation, sparse, graph, block Krylov-Schur algorithm, (1,2)-symmetric tensor, text analysis, traffic logs, spectral partitioning

**AMS subject classifications.** 05C50, 15A69, 65F15.

**1. Introduction.** Finding clusters in sparse data is a standard task in numerous areas of information sciences. Here we are concerned with data that are organized according to three categories, represented by real-valued tensors with three modes, i.e. objects  $\mathcal{A} \in \mathbb{R}^{l \times m \times n}$ . In particular we will be dealing with large, sparse tensors, which can be thought of as a collection of adjacency matrices for undirected graphs. Spectral partitioning is an important class of methods for finding interesting clustering structure in a graph, and extracting information from the data set represented by the graph. In this paper we present a method for analyzing tensors that can be considered as a generalization of spectral graph partitioning.

The proposed method is based on the computation of the best rank-(2,2,2) approximation of the tensor. This is the analogy with the computation of two eigenvalues and corresponding eigenvectors in spectral graph partitioning. By a reordering of certain vectors and applying the same reordering of the tensor, a clustering of the information in the tensor is performed. A variant of the method is also described, where an expansion of the tensor in rank-(2,2,1) terms is computed.

This paper is an investigation of the usefulness of the method in three application areas with large and sparse tensors. The first area is topic search in a collection of news texts from Reuters over 66 days. From this corpus of more than 13000 terms and their cooccurrence data organized in 66 graphs, we find the two main topics and their subtopics, and also analyze the topic variation in time. The clustering of the data tensor by the method is illustrated in Figure 1.1.

The second application is a tensor from a series of conferences, where the tensor modes represent authors, terms, and years. Our methods find the topics and their variation over the years. It also exhibits the development in time of participating authors.

The third data set is a tensor of network traffic logs over 371 time intervals, and the objective is to find the dominating senders (spammers?) and receivers out of

---

\*Department of Mathematics, Linköping University, Linköping, Sweden (lars.elden@liu.se)

†Department of Teleinformatics Engineering, Federal university of Ceará, Fortaleza, Brazil (maryamdehghan@ufc.br, maryamdehghan880@yahoo.com)

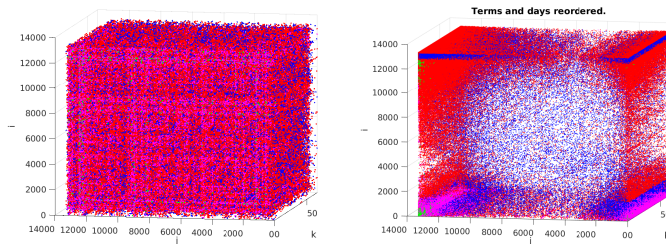


FIG. 1.1. *The original Reuters tensor (left) and reordered by our method (right). The two main topics are placed at the upper left and bottom right corners of the right plot. Each dot represents the cooccurrence of two terms in news texts from one day.*

almost 9000. We compute an approximation of the tensor in terms of an expansion of three rank-(2,1,1) terms, through which the dominating communication patterns are identified and visualized. In our fourth example we compute an expansion of seven rank-(2,2,1) terms of the above news text tensor. Each term in the expansion is a graph that represents a dominating topic and its prevalence during the time period.

This paper is the third in a series of three. In the first [13] we develop an algorithm for computing the best low-rank approximation of large and sparse tensors. The second paper [14] shows that the method used in the present paper can be considered as a generalization of spectral graph partitioning. The main contribution of the present paper is the demonstration that the best low-rank approximation can be used to analyze large and sparse tensor data coming from real applications.

More general purpose tensor clustering algorithms are described in [22, 25, 4, 31] and applied to synthetic examples and small to medium size examples with real data. Larger problems are solved in [5, 32].

This paper is organized as follows. We introduce some pertinent tensor concepts and give a very brief outline of our method in Section 2. Then in Section 3 we give more detailed description of the method of computing a best rank-(2,2,2) approximation as applied to the problem finding topics in news texts. The conference paper example is given in Section 4. The ideas behind the expansion of a tensor in rank-(2,2,1) terms are described in Section 5, and the application to the network traffic logs and topics in news texts in Section 5.2. The expansion algorithm is summarized in Section 5.3. Finally we give some concluding remarks in Section 6.

## 2. Tensor Concepts.

**2.1. Notation and Preliminaries.** Tensors will be denoted by calligraphic letters, e.g  $\mathcal{A}, \mathcal{B}$ , matrices by capital roman letters and vectors by lower case roman letters. In order not to burden the presentation with too much detail, we sometimes will not explicitly mention the dimensions of matrices and tensors, and assume that they are such that the operations are well-defined. The whole presentation will be in terms of tensors of order three, or equivalently 3-tensors. The generalization to order- $N$  tensors is obvious.

We will use the term tensor for a 3-dimensional array of real numbers,  $\mathcal{A} \in \mathbb{R}^{l \times m \times n}$ , where the vector space is equipped with some algebraic structures to be defined. The different “dimensions” of the tensor are referred to as *modes*. We will use both standard subscripts and “MATLAB-like” notation: a particular tensor element will be denoted in two equivalent ways,  $\mathcal{A}(i, j, k) = a_{ijk}$ .

A subtensor obtained by fixing one of the indices is called a *slice*, e.g.,  $\mathcal{A}(i, :, :)$ . In the case when the index is fixed in the first mode, we call the slice a 1-slice, and correspondingly for the other modes. A slice can be considered as an order-3 tensor (3-tensor) with a singleton mode, and also as a matrix. A tensor  $\mathcal{A}$  is called *(1,2)-symmetric* if all 3-slices  $\mathcal{A}(:, :, k)$  are symmetric. A *fiber* is a subtensor, where all indices but one are fixed. For instance,  $\mathcal{A}(i, :, k)$  denotes a mode-2 fiber.

For a given third order tensor, there are three associated subspaces, one for each mode. These subspaces are given by

$$\begin{aligned} &\text{Range}\{\mathcal{A}(:, j, k) \mid j = 1 : m, k = 1 : n\}, \\ &\text{Range}\{\mathcal{A}(i, :, k) \mid i = 1 : l, k = 1 : n\}, \\ &\text{Range}\{\mathcal{A}(i, j, :) \mid i = 1 : l, j = 1 : m\}. \end{aligned}$$

The *multilinear rank* [19, 9] of the tensor is said to be equal to  $(p, q, r)$  if the dimension of these subspaces are  $p, q$ , and  $r$ , respectively.

**2.2. Tensor-Matrix Multiplication.** We define *multilinear multiplication of a tensor by a matrix* as follows. For concreteness we first present multiplication by one matrix along the first mode and later for all three modes simultaneously. The mode-1 product of a tensor  $\mathcal{A} \in \mathbb{R}^{l \times m \times n}$  by a matrix  $U \in \mathbb{R}^{p \times l}$  is defined<sup>1</sup>

$$\mathbb{R}^{p \times m \times n} \ni \mathcal{B} = (U)_1 \cdot \mathcal{A}, \quad b_{ijk} = \sum_{\alpha=1}^l u_{i\alpha} a_{\alpha j k}. \quad (2.1)$$

This means that all mode-1 fibers in the 3-tensor  $\mathcal{A}$  are multiplied by the matrix  $U$ . Similarly, mode-2 multiplication by a matrix  $V \in \mathbb{R}^{q \times m}$  means that all mode-2 fibers are multiplied by the matrix  $V$ . Mode-3 multiplication is analogous. With a third matrix  $W \in \mathbb{R}^{r \times n}$ , the tensor-matrix multiplication in all modes is given by

$$\mathbb{R}^{p \times q \times r} \ni \mathcal{B} = (U, V, W) \cdot \mathcal{A}, \quad b_{ijk} = \sum_{\alpha, \beta, \gamma=1}^{l, m, n} u_{i\alpha} v_{j\beta} w_{k\gamma} a_{\alpha \beta \gamma}, \quad (2.2)$$

where the mode of each multiplication is understood from the order in which the matrices are given.

It is convenient to introduce a separate notation for multiplication by a transposed matrix  $\bar{U} \in \mathbb{R}^{l \times p}$ :

$$\mathbb{R}^{p \times m \times n} \ni \mathcal{C} = (\bar{U}^\top)_1 \cdot \mathcal{A} = \mathcal{A} \cdot (\bar{U})_1, \quad c_{ijk} = \sum_{\alpha=1}^l a_{\alpha j k} \bar{u}_{\alpha i}. \quad (2.3)$$

Let  $u \in \mathbb{R}^l$  be a vector and  $\mathcal{A} \in \mathbb{R}^{l \times m \times n}$  a tensor. Then

$$\mathbb{R}^{1 \times m \times n} \ni \mathcal{B} := (u^\top)_1 \cdot \mathcal{A} = \mathcal{A} \cdot (u)_1 \equiv B \in \mathbb{R}^{m \times n}. \quad (2.4)$$

Thus we identify a tensor with a singleton dimension with a matrix.

<sup>1</sup>The notation (2.1)-(2.2) was suggested by de Silva and Lim [9]. An alternative notation was earlier given in [7]. Our  $(X)_d \cdot \mathcal{A}$  is the same as  $\mathcal{A} \times_d X$  in the latter system.

**2.3. Inner Product and Norm.** Given two tensors  $\mathcal{A}$  and  $\mathcal{B}$  of the same dimensions, we define the *inner product*,

$$\langle \mathcal{A}, \mathcal{B} \rangle = \sum_{\alpha, \beta, \gamma} a_{\alpha\beta\gamma} b_{\alpha\beta\gamma}, \quad (2.5)$$

and the analogous for 2-tensors. The corresponding *tensor norm* is

$$\|\mathcal{A}\| = \langle \mathcal{A}, \mathcal{A} \rangle^{1/2}. \quad (2.6)$$

This *Frobenius norm* will be used throughout the paper. As in the matrix case, the norm is invariant under orthogonal transformations, i.e.

$$\|\mathcal{A}\| = \|(U, V, W) \cdot \mathcal{A}\| = \|\mathcal{A} \cdot (P, Q, S)\|,$$

for orthogonal matrices  $U, V, W, P, Q$ , and  $S$ . This is obvious from the fact that multilinear multiplication by orthogonal matrices does not change the Euclidean length of the corresponding fibers of the tensor.

**2.4. Best Rank- $(r_1, r_2, r_3)$  Approximation.** The problem of approximating tensor  $\mathcal{A} \in \mathbb{R}^{l \times m \times n}$  by another tensor  $\mathcal{B}$  of lower multi-linear rank,

$$\min_{\text{rank}(\mathcal{B})=(r_1, r_2, r_3)} \|\mathcal{A} - \mathcal{B}\|^2, \quad (2.7)$$

is treated in [8, 34, 15, 20]. It is shown in [8] that (2.7) is equivalent to

$$\max_{X, Y, Z} \|\mathcal{A} \cdot (X, Y, Z)\|^2, \quad \text{subject to} \quad X^\top X = I_{r_1}, \quad Y^\top Y = I_{r_2}, \quad Z^\top Z = I_{r_3}, \quad (2.8)$$

where  $X \in \mathbb{R}^{l \times r_1}$ ,  $Y \in \mathbb{R}^{m \times r_2}$ , and  $Z \in \mathbb{R}^{n \times r_3}$ . The problem (2.8) can be considered as a *Rayleigh quotient maximization problem*, in analogy with the matrix case [2]. To simplify the terminology somewhat we will refer to a solution  $(U, V, W)$  of the approximation problem as *the best rank- $(r_1, r_2, r_3)$  approximation of the tensor*; it is straightforward to prove [8] that the corresponding core tensor is  $\mathcal{F} = \mathcal{A} \cdot (U, V, W)$ , so, strictly speaking,  $\mathcal{B} = (U, V, W) \cdot \mathcal{F}$  is the best approximation. In the case when the tensor is (1,2)-symmetric, the solution has the form  $(U, U, W)$ , cf. [14].

The constrained maximization problem (2.8) can be thought of as an unconstrained maximization problem on the *Grassmann manifold*, cf. [11, 1, 15].

**2.5. Computing the Best Low-Rank Approximation.** The simplest algorithm for computing the best low-rank approximation of a tensor is the HOOI method, which is an alternating orthogonal iteration algorithm [8]. For small and medium-size tensors Grassmann variants of standard optimization algorithms often converge faster [20, 15, 28, 21]. For large and sparse tensors a block Krylov-Schur-like (BKS) method has been developed [13]. It is analogous to an algorithm [24], which is a standard method for computing a low-rank approximation of matrices. The method is memory efficient as it uses the tensor only in tensor-matrix multiplications, where the matrix has a small number of columns. Convergence is often quite fast for tensors with data from applications. It is shown in [13] that the BKS method is more robust and faster than HOOI for large and sparse tensors, and we use it throughout this paper.

**2.6. Partitioning Graphs by Low-Rank Approximation.** Spectral partitioning is a standard method for partitioning undirected graphs that are close to being disconnected, see e.g. [26, 6, 30, 27]. Often it is based on the computation of the two smallest eigenvalues of the normalized graph Laplacian. We here give a brief account of the equivalent approach (see e.g. [12, Chapter 10]), when the two largest eigenvalues of the normalized adjacency matrix are used. Let the adjacency matrix be  $A$  and the degree matrix,  $D = \text{diag}(d) = \text{diag}(Ae)$ , where  $e$  is a vector of all ones. The normalized adjacency matrix

$$A_N = D^{-1/2} A D^{-1/2} \quad (2.9)$$

has largest eigenvalue equal to 1. If the graph is connected, then the second largest eigenvalue is strictly smaller than 1, and the corresponding eigenvector, the Fiedler vector, can be used to partition the graph into two subgraphs so that the cost (essentially in terms of the number of broken edges) is small. The eigenvectors  $u_1$  and  $u_2$  of the Karate club graph [33], see also [12, Chapter 10], are illustrated in Figure 2.1.

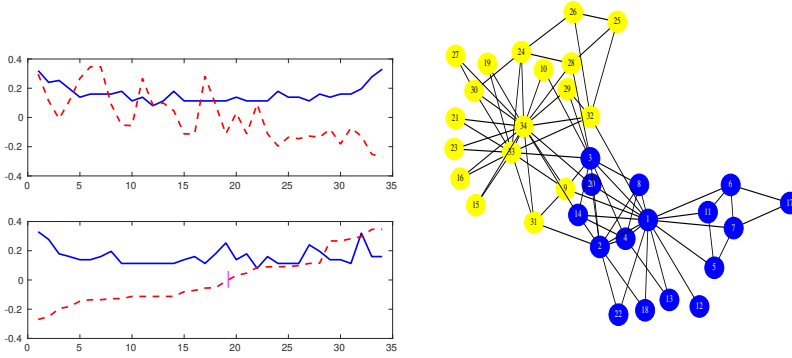


FIG. 2.1. The first two eigenvectors  $u_1$  (blue, solid) and  $u_2$  (red, dashed) of the normalized adjacency matrix of the Karate club graph, original (top left) and reordered (bottom left). The magenta vertical line shows the position, where the elements of reordered vector  $u_2$  changes sign. Partitioning the reordered vertices in the neighborhood of the sign change gives a low cost in terms of the number of broken edges, see [12, Chapter 10]. The right panel shows the partitioned graph (colorcoded).

In [14] spectral graph partitioning is generalized to (1,2)-symmetric tensors, where each 3-slice can be considered as the normalized adjacency matrix of an undirected graph. A concept of disconnectedness of tensors is defined, and it is shown that (1,2)-symmetric tensors that are close to being disconnected can be partitioned so that the partitioning cost is small. The partitioning is derived from the best rank-(2,2,2) approximation  $(U, U, W)$  of the tensor. The partitioning procedure is analogous to the matrix case, and we describe it in connection with the example in Section 3. For further details, see [14].

In Section 4 we partition a tensor that is non-symmetric. The method is analogous to the (1,2)-symmetric case. Here a non-symmetric scaling of the 3-slices is used [10].

**3. Topic search in News Text.** The data for this example are described in [3]. We cite from the description:<sup>2</sup>

<sup>2</sup><http://vlado.fmf.uni-lj.si/pub/networks/data/CRA/terror.htm>.

“The *Reuters terror news network* is based on all stories released during 66 consecutive days by the news agency Reuters concerning the September 11 attack on the U.S., beginning at 9:00 AM EST 9/11/01. The vertices of a network are words (terms); there is an edge between two words iff they appear in the same text unit (sentence). The weight of an edge is its frequency. The network has  $n = 13332$  vertices (different words in the news) and  $m = 243447$  edges, 50859 with value larger than 1. There are no loops in the network.”

We organized the data in a tensor  $\mathcal{A} \in \mathbb{R}^{13332 \times 13332 \times 66}$ , where each 3-slice was normalized as in (2.9). Thus  $a_{ijk} > 0$  if terms  $i$  and  $j$  occur in the same sentence in the news during day  $k$ ; otherwise  $a_{ijk} = 0$ . Each 3-slice is the normalized adjacency matrix of an undirected graph, and the tensor is (1,2)-symmetric. The tensor is illustrated to the left in Figure 1.1. Each nonzero element is shown as a colored dot. The horizontal and vertical directions correspond to terms, and the lateral directions to days. The color coding is from blue for the largest elements, via red and magenta to green for the smallest non-zero elements. The same coding is used in all similar figures. Due to the fact that several non-zeros can be hidden behind others, the coding is more informative when the tensor is relatively small or has some larger scale structure (as in the following figures). The code for producing the plot is a modification of `spy3` from Tensorlab<sup>3</sup>. Obviously it is impossible to discern any useful structure from the image of the tensor.

In spectral graph partitioning (Section 2.6) we compute the two largest eigenvalues and corresponding eigenvectors of the normalized adjacency matrix, which is equivalent to computing the best rank-2 approximation of the matrix. The analogous concept for a (1,2)-symmetric tensor is the best rank-(2,2,2) approximation of the tensor, which we computed using the BKS method<sup>4</sup>. Since the problem is (1,2)-symmetric, we have  $U = V$ . The elements of the column vectors of  $U$ , which we call term vectors, are reordered so that those of  $U(:, 2)$  become monotonic; we refer to the reordered term vectors as  $(u_1, u_2)$ . Similarly the elements of the column vectors of  $W$  are reordered, giving the day vectors  $(w_1, w_2)$ . The vectors for the Reuters tensor are illustrated in Figure 3.1. A closer look (using a logarithmic plot) at the middle elements, 9000 say, of  $u_1$  reveals that they are at least a couple of magnitudes smaller than the elements at the beginning and the end. This indicates that the middle elements are insignificant in the mode-(1,2) partitioning of the tensor; analogously, the corresponding terms are insignificant in the search for topics. In Table 3.1 we list the 25 first and last reordered terms, as well as 25 close to the sign change of  $u_2$ . It is apparent from the table that we have two different topics, which we will refer to as  $T^1$  and  $T^2$ .

Applying the same reordering to the original tensor, we get the tensor illustrated in Figure 3.2. It is seen that the “mass” is concentrated to the four corners in term modes, which correspond to Topics 1 and 2 in Table 3.1. We computed the norms of the subtensors of dimensions  $1000 \times 1000 \times 66$  at the corners, and they were 50.6, 25.5, 25.5, and 35.1, respectively. As the norm of  $\mathcal{A}$  was 128.6, 15% of the terms accounted for about 55% of the total mass.

The relatively dense cluster at the top left in Figure 3.2 shows that the terms from topic  $T^2$  cooccur to a great extent with other terms from  $T^2$ . Looking at the bottom right cluster, the analogous statement can be made about topic  $T^1$ . The cluster at

<sup>3</sup><https://www.tensorlab.net/>

<sup>4</sup>The execution time in Matlab on a standard desk top computer was about 44 seconds.

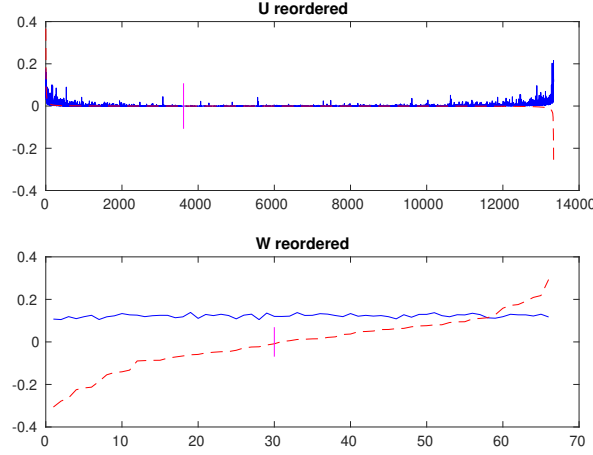


FIG. 3.1. The column vectors of  $U$  and  $W$  after reordering;  $u_1$  and  $w_1$  are blue and the others red. The magenta vertical lines show the position, where the elements of reordered vectors  $u_2$  and  $w_2$  change sign.

TABLE 3.1

Beginning terms, middle terms and end terms after reordering. The table is organized so that the most significant terms appear at the top of the first column and the bottom of the third (to conform with the image of the reordered tensor in Figure 3.2). The middle column shows a few terms at the middle, which are relatively insignificant with respect to the topics in the other two columns.

$T^1$	Insignificant	$T^2$
world_trade_ctr	planaria	hand
pentagon	mars	ruler
new_york	i.d	saudi
attack	eyebrow	guest
hijack	calendar	mullah
plane	belly	movement
airliner	auction	camp
tower	attentiveness	harbor
twin	astronaut	shelter
washington	ant	group
sept	alligator	organization
suicide	adjustment	leader
pennsylvania	cnd	rule
people	nazarbayev	exile
passenger	margrit	guerrilla
jet	bailes	afghanistan
mayor	newscast	fugitive
110-story	turgan-tiube	dissident
mayor_giuliani	N52000	taliban
hijacker	ishaq	islamic
commercial	sauce	network
aircraft	sequential	al_quaeda
assault	boehlert	militant
airplane	tomato	saudi-born
miss	resound	bin_laden

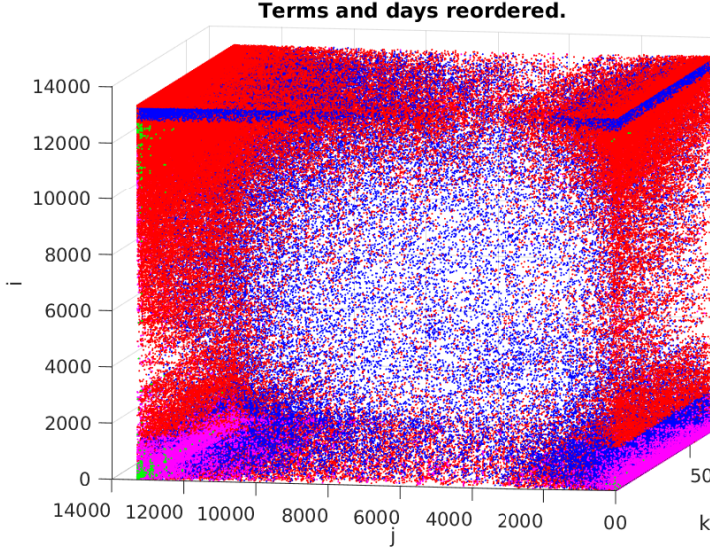


FIG. 3.2. The tensor reordered in the term and day modes. The top left terms correspond to those in the first column in Table 3.1, and the bottom right terms to those in the third column of Table 3.1. It is interesting to note that many of the insignificant terms at the middle of the tensor in the figure are marked blue. This indicates that even if those terms are insignificant they are rather frequent.

the top right in the tensor indicates that many terms from topic  $T^1$  cooccur with those in  $T^2$ . Apart from this, it is not possible to discern in Figure 3.2 any interesting structure.

To check that the middle terms are insignificant, we removed approximately 9000 middle terms (after the reordering), and computed a best rank-(2,2,2) approximation of a tensor of dimension  $4333 \times 4333 \times 66$ . The analysis gave exactly the same most significant terms as in the first and third columns of Table 3.1.

We divided the 66 days into two groups, where the first,  $D_A$  (30 days), corresponds to the (original) indices of  $w_2$  to the left of the sign change, see Figure 3.1. The second group,  $D_B$  (36 days), corresponds to the (original) indices to the right. It turns out that the reordered days are not consecutive:

```
DA: XXXXXXXXXXXX X XX X XX XX X XX XXX X X X X X X
DB: X XX X XX X XXXX X XXXXXXXXXXXX XX X X X XXX X XXX
```

To see if there is any difference in vocabulary during the groups of days,  $D_A$  and  $D_B$ , we analyzed the groups separately, by computing the best rank-(2,2,2) approximations of the tensors  $\mathcal{A}(:, :, D_A) \in \mathbb{R}^{13332 \times 13332 \times 30}$  and  $\mathcal{A}(:, :, D_B) \in \mathbb{R}^{13332 \times 13332 \times 36}$ . The reordered tensors are shown in Figure 3.3, and the most significant terms in Table 3.2.

From Table 3.2 we see that the topics are similar for days  $D_A$  and  $D_B$ , but the terms used differ considerably. In addition, Figure 3.3 shows that the vocabulary used for topic  $T^1$  is much more concentrated during  $D_A$  than during  $D_B$ . The opposite is true of topic  $T^2$ . It is also seen that the number of insignificant terms that are not used at all, or used very infrequently, during  $D_A$  and  $D_B$  are about 3200 and 4800, respectively.



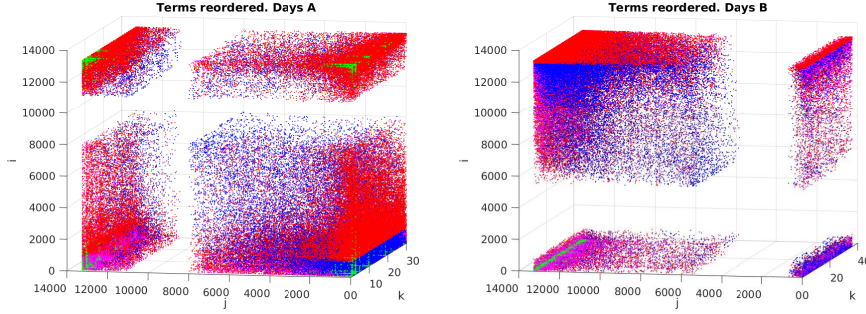


FIG. 3.3. Top row: The tensors for  $D_A$  and  $D_B$  reordered separately in the term mode.

TABLE 3.2

The topics of the two groups of days. The most significant terms appear at the top of the left two columns and at the bottom of the right two.

$T_A^1$	$T_B^1$	$T_A^2$	$T_B^2$
world_trade_ctr	attack	country	hand
tower	world_trade_ctr	muslim	millionaire
pentagon	new_york	force	pakistan-based
twin	pentagon	united_states	leader
new_york	hijack	ruler	movement
plane	united_states	reuter	follower
hijack	anthrax	law	saudi
airliner	tell	mullah	guest
attack	plane	pakistan	group
110-story	people	network	harbor
washington	airliner	dissident	train
pennsylvania	washington	terrorism	camp
commercial	reuter	group	organization
passenger	official	military	taliban
jet	sept	tell	exile
mayor	reporter	war	shelter
suicide	city	al_quaeda	guerrilla
hijacker	news	leader	dissident
mayor_giuliani	suicide	islamic	islamic
ruin	worker	militant	fugitive
rural	security	rule	network
crash	office	afghanistan	al_quaeda
rubble	day	saudi-born	militant
people	tower	taliban	saudi-born
flight	letter	bin_laden	bin_laden

It is possible to apply the procedure recursively: As an example, we took the subtensor of dimension  $7333 \times 7333 \times 36$  at the top left of the right image in Figure 3.3, that contains mainly terms from topic  $T^1$  during days  $D_B$ , and computed its best rank-(2,2,2) approximation. This produced the two subtopics given in Table 3.3.

It is necessary to ask the question if the tensor method gives more information than an analogous spectral matrix/graph analysis. To investigate this, we computed

TABLE 3.3

Two subtopics of topic  $T_B^1$ . The most significant terms appear at the top of the first column and at the bottom of the fourth. It is seen that the two left columns are somewhat more “politically” oriented, while the two right columns are concerned with the actual attack.

$T_B^{11}$		$T_B^{12}$	
tell	special	jet	tower
reuter	foreign	people	september
reporter	war	airplane	washington
force	news	month	suicide
northern_alliance	military	wake	plane
opposition	security	assault	sept
rumsfeld	defense	passenger	airliner
official	pakistan	11	new_york
sec	united_states	devastate	pentagon
pres_bush	conference	hijacker	hijack
kabul	terrorism	pennsylvania	attack
minister	government	twin	world_trade_ctr

a matrix by adding all the 3-slices of the tensor and then normalizing as in (2.9). This is the normalized adjacency matrix of the graph that has an edge between two terms if they occur in the same sentence any time during the 66 days, weighted by the number of occurrences. Spectral partitioning using the reordered eigenvector corresponding to the second largest eigenvalue gives mixed terms from topics  $T^1$  and  $T^2$  at one end, and seemingly random, insignificant terms at the other. Thus the matrix approach does not separate the terms from topics  $T^1$  and  $T^2$ . We repeated the experiment, where we removed about 8000 insignificant terms. The results were very similar to those with the full data set.

**4. NeurIPS Conference Papers.** Experiments with data from all the papers at the Neural Information Processing Systems Conferences<sup>5</sup> 1987-2003 are described in [17]. We downloaded the data from <http://frostdt.io/> [29], and formed a sparse tensor of dimension  $2862 \times 14036 \times 17$ , where the modes represent (author, terms, year), and the values are term counts. We performed a non-symmetric normalization of the 3-slices of the tensor. The tensor is illustrated in Figure 4.1.

Then we computed the best rank-(2,2,2) approximation of the tensor and reordered the vectors as in the example in Section 3, see Figure 4.2. The tensor reordered in the author and term modes is illustrated in Figure 4.1. Some structure can be seen, but not very clearly. The reordered term vector suggests that the two main topics in the conferences during years 1-17 are those given in Table 4.1.

From the spy-plot of the tensor in Figure 4.1 (right), we see structure in the time-author modes. The reordering of the year vector is

4 6 3 5 2 7 1 8 9 10 11 12 13 14 17 15 16

This indicates (as expected) that the structure differs between the first and the last years of the period. To investigate that we analyzed separately the tensors for years 1-9, and 10-17.

In Figure 4.3 we illustrate the reordered tensor for years 1-9. The gap in the

<sup>5</sup>The acronym for the conferences used to be NIPS, but in 2018 it was changed to NeurIPS. We will use the latter.

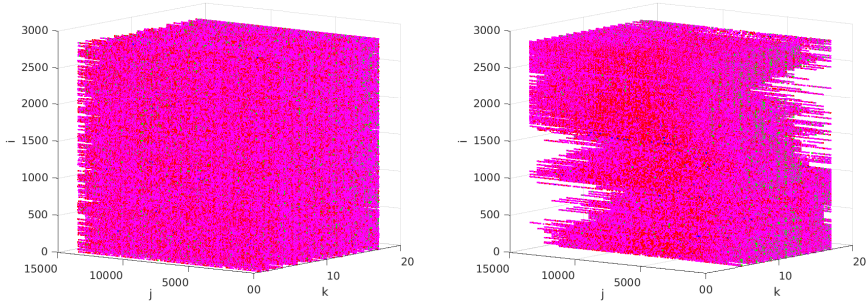


FIG. 4.1. Left: Original NeurIPS tensor. The author mode is vertical, the term mode is horizontal, and the year mode is lateral. The same color coding as in the previous section is used. Right: Reordered NeurIPS tensor. The tensor is reordered in the author and term modes.

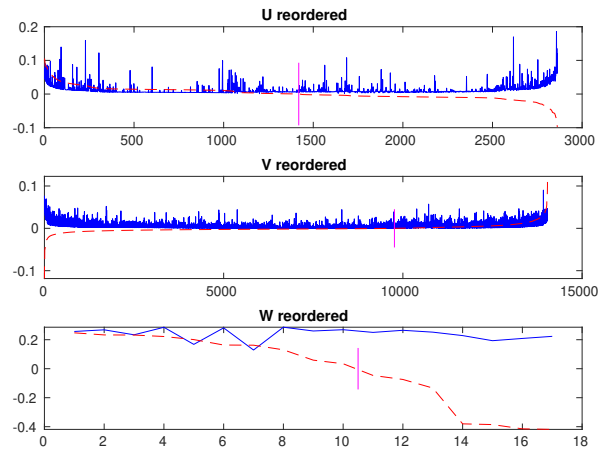


FIG. 4.2. Reordered vectors in the best rank-(2,2,2) approximation of the NeurIPS tensor.

TABLE 4.1

Two main topics at NeurIPS conferences during years 1-17. The terms are ordered so that the most important are at the top of column 1 and at the bottom of column 4.

$T^1$		$T^2$	
network	error	flies	neurobiology
learning	figure	individuals	jerusalem
training	layer	independence	van
input	weights	princeton	steveninck
units	time	engineering	bialek
networks	set	huji	william
output	algorithm	israel	code
model	function	hebrew	rob
state	hidden	center	tishby
weight	signal	ruyter	brenner
performance	image	school	naftali
recognition	unit	nec	universality

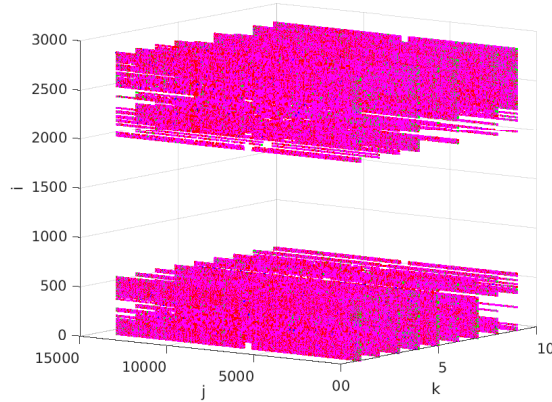


FIG. 4.3. The tensor for the years 1-9, reordered in the author and term modes.

middle of Figure 4.3 corresponds to authors who were not present during years 1-9. The main topics are given in Table 4.2.

TABLE 4.2  
Two main topics at NeurIPS conferences during years 1-9 (denoted  $A$ ).

$T_A^1$		$T_A^2$	
propagation	neuron	schraudolph	mixtures
units	hopfield	eye	gamma
back	patterns	jabri	gesture
connections	pattern	reward	policy
network	layer	leen	singh
analog	chips	pca	mixture
chip	fig	density	jordan
connection	hidden	experts	model
synapse	classifiers	validation	tresp
circuit	parallel	prediction	missing
bower	vowel	data	em
associative	input	tangent	dayan

We made the same analysis for years 10-17. The results are given in Figure 4.4 and Table 4.3. In the left panel of Figure 4.4 we can see that there are more authors in the years 10-17. In the right panel we have used the same author ordering as in Figure 4.3. The new authors, who did not contribute during the years 1-9, are seen at the middle of the spy-plot. It is also clear that many of the authors from years 1-9 are not present, see the slightly thinner pattern at the top and bottom.

Comparing Tables 4.1 and 4.3 we see that it is the topics of the last 8 years that dominate for the whole period. The neural network topic is, of course, the most significant one during the whole period, but note that one can see slight differences between Tables 4.2 and 4.3.

**5. Approximating (1,2)-Symmetric Tensors by an Expansion of Rank-(2,2,1) Terms.** In some applications the purpose of the analysis is to find dominating patterns in tensor data. In the network traffic example in Section 5.1 below there

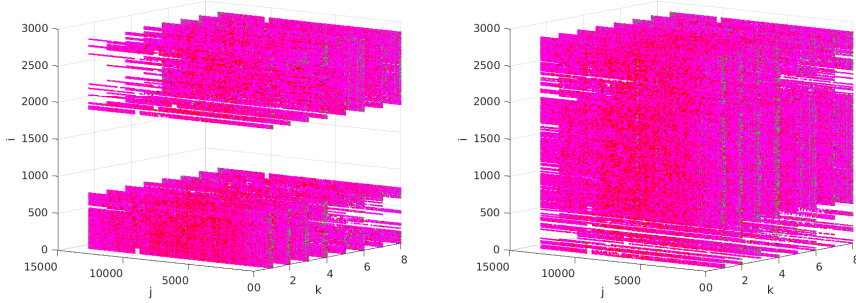


FIG. 4.4. Left: The tensor for the years 10-17, reordered in the author and term modes. Right: The same tensor, but the authors (vertical mode) have been ordered as in Figure 4.3.

TABLE 4.3

Two main topics at NeurIPS conferences during years 10-17 (denoted  $B$ ).

$T_B^1$		$T_B^2$	
model	models	usa	center
learning	figure	flies	school
algorithm	vector	independence	nec
training	error	israel	bialek
data	input	engineering	steveninck
network	case	huji	code
function	number	hebrew	william
state	em	princeton	rob
noise	likelihood	ruyter	tishby
set	functions	van	brenner
networks	probability	jerusalem	naftali
gaussian	class	neurobiology	universality

are ip-addresses, from which many malicious attacks are sent to a large number of target addresses. The data are organized as a temporal sequence of graphs that represent communication between ip-addresses. In order to identify the attackers one needs to find dominating subgraphs. Also, it may be interesting to study temporal communication patterns.

We assume that the nonnegative tensor  $\mathcal{A} \in \mathbb{R}^{m \times m \times n}$  is  $(1, 2)$ -symmetric and that the third mode is the temporal mode: each 3-slice  $\mathcal{A}(:, :, k)$  is the adjacency matrix of an undirected communication graph. Our analysis is based on Proposition 5.1, proved in [14]. Let  $\mathcal{C} \in \mathbb{R}^{m_1 \times m_2 \times n}$ , and define  $\mathcal{C}' \in \mathbb{R}^{m_2 \times m_1 \times n}$  to be the tensor such that each 3-slice is the transpose of the corresponding slice in  $\mathcal{C}$ .

PROPOSITION 5.1. *Let the  $(1, 2)$ -symmetric, nonnegative tensor  $\mathcal{A} \in \mathbb{R}^{m \times m \times n}$  have the structure*

$$\mathcal{A} = \begin{pmatrix} 0 & \mathcal{C} \\ \mathcal{C}' & 0 \end{pmatrix}, \quad \mathcal{C} \in \mathbb{R}^{m_1 \times m_2 \times n}, \quad m_1 + m_2 = m.$$

*Assume that the best rank- $(1, 1, 1)$  approximation of  $\mathcal{C}$  is unique, given by nonnegative*

$(u, v, w)$ , and let  $\mathcal{C} \cdot (u, v)_{1,2} = \tau w$ , where  $\tau > 0$ . Define the matrix  $U$ ,

$$U = \begin{pmatrix} 0 & u \\ v & 0 \end{pmatrix}. \quad (5.1)$$

Then the best rank-(2, 2, 1) approximation of  $\mathcal{A}$  is given by  $(U, U, w)$ , and

$$\mathbb{R}^{2 \times 2 \times 1} \ni \mathcal{F} = \begin{pmatrix} 0 & \tau \\ \tau & 0 \end{pmatrix}.$$

The rank-(2, 2, 1) approximation  $(U, U, w) \cdot \mathcal{F}$  can be written

$$(U, U, w) \cdot \mathcal{F} = (w)_3 \cdot \mathcal{B}, \quad \mathcal{B} = (U, U)_{1,2} \cdot \mathcal{F} \in \mathbb{R}^{m \times m \times 1},$$

where  $\mathcal{B}$  can be identified with a matrix  $B \in \mathbb{R}^{m \times m}$ . We can also write

$$B = \hat{U} \hat{F} \hat{U}^T, \quad \hat{U} = \frac{1}{\sqrt{2}} \begin{pmatrix} u & -u \\ v & v \end{pmatrix}, \quad \hat{F} = \begin{pmatrix} \tau & 0 \\ 0 & -\tau \end{pmatrix}. \quad (5.2)$$

It is easy to see that if we embed  $\mathcal{C}$  symmetrically in a larger *zero tensor*  $\mathcal{Z} \in \mathbb{R}^{M \times M \times n}$ , with  $M > m$ , then the corresponding results hold. Let the solution of the best rank-(2, 2, 1) approximation for  $\mathcal{Z}$  be  $(U_0, U_0, w_0)$ , which consists of the elements of  $(U, U, w)$  embedded in larger zero matrices and vectors. Furthermore, if we embed  $\mathcal{C}$  symmetrically in a larger (1,2)-symmetric but nonnegative tensor  $\mathcal{A}_0 \in \mathbb{R}^{M \times M \times n}$ , which has much smaller norm,  $\|\mathcal{A}_0\| \ll \|\mathcal{C}\|$ , then since the best approximation depends continuously on the elements of the tensor [16], the solution of the best rank-(2, 2, 1) approximation problem for  $\mathcal{A} = \mathcal{A}_0 + \mathcal{C}$  will be

$$(U, U, w) = (E, E, e) + (U_0, U_0, w_0), \quad \|(E, e)\| \approx K \|\mathcal{C}\| / \|\mathcal{A}\|,$$

where  $E$  and  $e$  are perturbations, and  $K$  depends on the conditioning of the approximation problem for  $\mathcal{A}$  [16]. The estimate is essentially the same as when we compute a best rank-1 approximation of a matrix (principal components, singular value decomposition). This implies that we can use the best rank-(2, 2, 1) approximation to determine the dominating information in a data tensor.

In the matrix SVD case, due to the fact that the singular value decomposition diagonalizes the matrix, we get the best rank-1, rank-2, rank-3, etc. approximations directly from the SVD, see, e.g., [12, Chapter 6], [18, Chapter 2]. The corresponding is not the case for the best rank- $(r_1, r_2, r_3)$  approximation of a tensor. Therefore, we suggest a procedure, where we explicitly deflate the tensor<sup>6</sup>. Assuming that the best rank-(2,2,1) approximation of the tensor  $\mathcal{R}^{(1)} := \mathcal{A}$  is given by  $(U^{(1)}, U^{(1)}, w^{(1)})$ , with core tensor  $\mathcal{F}^{(1)}$  and  $B^{(1)} = (U^{(1)}, U^{(1)})_{1,2} \cdot \mathcal{F}^{(1)}$ , we compute

$$\mathcal{R}^{(2)} := \mathcal{R}^{(1)} - (w^{(1)})_3 \cdot B^{(1)}.$$

Repeating this process, i.e. computing a rank-(2,2,1) approximation of  $\mathcal{R}^{(\nu)}$ ,  $\nu = 2, 3, \dots$ , and putting  $\mathcal{R}^{(\nu+1)} = \mathcal{R}^{(\nu)} - (w^{(\nu)})_3 \cdot B^{(\nu)}$ , then after  $q - 1$  steps we have an expansion

$$\mathcal{A} = \sum_{\nu=1}^q (w^{(\nu)})_3 \cdot B^{(\nu)} + \mathcal{R}^{(q)}.$$

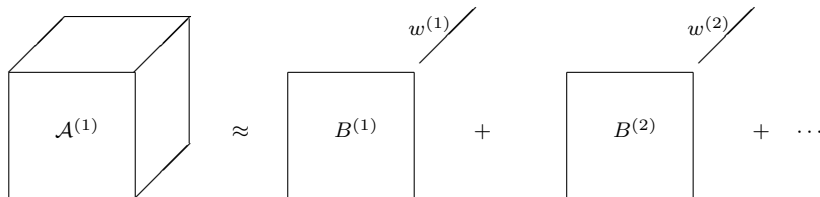


FIG. 5.1. Symbolic illustration of the rank-(2,2,1) expansion of a tensor.

Clearly the matrices  $B^{(\nu)}$  have rank 2, so we can call the expansion a *rank-(2,2,1) expansion*. The expansion is illustrated symbolically in Figure 5.1. We present further details of the algorithm in connection with an example in Section 5.1. There the expansion is applied to a nonnegative and sparse tensor, which has dominating patterns, so for this tensor the motivation above is applicable. However, in order to avoid destroying sparsity and nonnegativity modifications of the procedure are introduced.

The example described in Section 5.2, does not have that property of strongly dominating patterns, i.e., the eigenvalues of the matrices  $F^{(\nu)}$  do not appear in pairs with different signs. Still the expansion gives meaningful results.

The algorithm is summarized in Section 5.3. There we also point out the features of the algorithm that ensure that for sparse, nonnegative tensors, the expansion is also sparse and nonnegative.

**5.1. Rank-(2,2,1) Expansion of Network Traffic Logs.** In [23] network traffic logs are analyzed in order to identify malicious attackers. The data are called the 1998 DARPA Intrusion Detection Evaluation Dataset and were first published by the Lincoln Laboratory at MIT<sup>7</sup>. We downloaded the data set from <https://datalab.snu.ac.kr/haten2/> in October 2018. The records consist of (source IP, destination IP, port number, timestamp). In the data file there are about 22000 different IP addresses. We chose the subset of 8991 addresses that both sent and received messages. The time span for the data is from June 1 1998 to July 18, and the number of observations is about 23 million. We merged the data in time by collecting every 63999 consecutive observations into one bin. Finally we symmetrized the tensor  $\mathcal{A} \in \mathbb{R}^{m \times m \times n}$ , where  $m = 8991$  and  $n = 371$ , so that

$$a_{ijk} = \begin{cases} 1 & \text{if } i \text{ communicated with } j \text{ in time slot } k \\ 0 & \text{otherwise.} \end{cases}$$

In this example we did not normalize the slices of the tensor: The 3-slices are extremely sparse, and normalization makes the rank-(2,2,1) problem so ill-conditioned that the BKS algorithm did not converge. Instead we scaled the slices to have Frobenius norm equal to 1. This problem is very well-conditioned and the Krylov-Schur algorithm converged in 5 iterations. We refer to this as the 1998DARPA tensor, and it is illustrated in Figure 5.2. For this type of data one relevant task is to identify the dominating IP addresses, that communicate with many others. These may be spammers. We will now demonstrate how we can extract such information by computing

<sup>6</sup>In the matrix case a similar procedure would give the SVD.

<sup>7</sup><http://www.ll.mit.edu/r-d/datasets/1998-darpa-intrusion-detection-evaluation-dataset>.

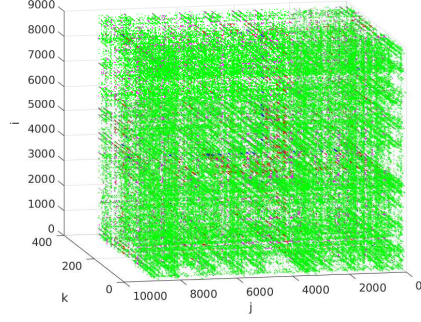


FIG. 5.2. 1998DARPA tensor, original ordering.

the rank-(2, 2, 1) approximation of the tensor. The  $U^{(1)} = (u_1^{(1)} u_2^{(1)})$  and  $w^{(1)}$  vectors are shown in Figure 5.3. The core tensor was

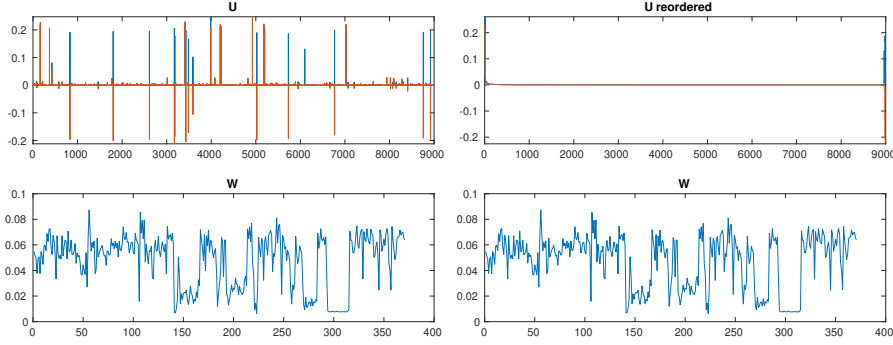


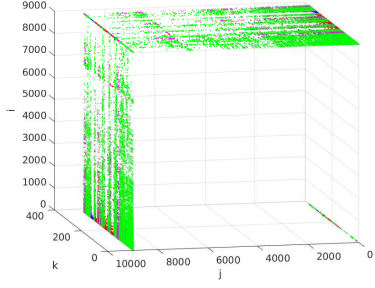
FIG. 5.3. Top panels: the vectors  $u_1^{(1)}$  (blue),  $u_2^{(1)}$  (red). Bottom panels:  $w^{(1)}$ . Left: Original ordering. Right:  $(u_1^{(1)} u_2^{(1)})$  are reordered so that the elements of  $u_2^{(1)}$  are monotonically decreasing.

$$\mathcal{F}^{(1)} = \begin{pmatrix} 6.35 & 0 \\ 0 & -6.12 \end{pmatrix}.$$

We chose to diagonalize  $F^{(1)}$  and transform  $U^{(1)}$  accordingly, see (5.2). The rank-(2, 2, 1) approximation accounted for quite a large part of  $\mathcal{A}$ :  $\|\mathcal{A}\| \approx 19.26$  and  $\|\mathcal{F}^{(1)}\| \approx 8.82$ .

The  $U^{(1)}$  vectors are very sparse and spiky, which indicates that very few addresses are dominating the communication. When we reordered so that  $u_2^{(1)}$  became monotonically decreasing, the most active addresses (the spikes) are placed at the beginning and the end. Applying the same reordering to the tensor in the (1,2)-modes, we got the left panel in Figure 5.4. In the sequel, for notational convenience, we let  $\mathcal{A}$  denote the reordered tensor and  $U^{(1)}$  the correspondingly reordered matrix. Clearly there is a relatively small group of addresses (upper left corner in Figure 5.4) that communicate with the majority of the others, and another very small group (lower right corner) that communicate only within the small group and with the first group (upper right corner). The majority of addresses (middle) do not communicate with each other.





$$\begin{bmatrix} 2.77 & 7.83 & 10.92 \\ 7.83 & 0.11 & 0 \\ 10.92 & 0 & 1.48 \end{bmatrix}$$

FIG. 5.4. 1998DARPA tensor, reordered in the  $(1,2)$  modes. Right: Norms of tensor blocks  $\mathcal{A}(I, J, :)$ , where  $I$  and  $J$  are sequences of indices, such that the outermost blocks are 100 elements wide.

As the columns of  $U^{(1)}$  are orthogonal, we can not expect the matrix  $B^{(1)} = (U^{(1)}, U^{(1)})_{1,2} \cdot \mathcal{F}^{(1)}$  to be sparse; in this example it even has small negative elements (the smallest element of  $B^{(1)}$  is  $-0.018$  and the largest is  $0.63$ ). In order to have a sparse and nonnegative approximation we define a new matrix  $\hat{B}^{(1)}$ : we let  $b_{\max}$  be the largest element in  $B^{(1)}$ , and for  $\theta = 0.01$  we put

$$\hat{b}_{ij}^{(1)} = \begin{cases} b_{ij}^{(1)} & \text{if } b_{ij}^{(1)} > \theta b_{\max}, \\ 0, & \text{otherwise.} \end{cases} \quad (5.3)$$

Thus we approximated

$$\mathcal{R}^{(1)} := \mathcal{A} = \left(w^{(1)}\right)_3 \cdot \hat{B}^{(1)} + \mathcal{R}^{(2)},$$

where  $\mathcal{R}^{(2)}$  is a residual tensor. The approximation is illustrated in Figures 5.5 and 5.6. Note that the low rank approximation is concentrated in this blocks where the reordered tensor has highest “density”, cf. Figure 5.4.

The addresses that dominate the communication can be identified in the matrix  $\hat{B}^{(1)}$ . In fact,  $\hat{B}^{(1)}$  can be interpreted as the adjacency matrix of a communication graph for the dominating communication, and the vector  $w_1^{(1)}$  (Figure 5.3) shows the strength of the communication at the different time slots.

Next we deflated the tensor,

$$\mathcal{R}^{(2)} = \mathcal{R}^{(1)} - \left(w^{(1)}\right)_3 \cdot \hat{B}^{(1)}.$$

The deflated tensor is illustrated in Figure 5.7. We performed the same analysis on  $\mathcal{R}^{(2)}$  with the analogous thresholding for  $\hat{B}^{(2)}$ . The core tensor was

$$\mathcal{F}^{(2)} = \begin{pmatrix} -5.09 & 0 \\ 0 & 5.12 \end{pmatrix}.$$

The rank- $(2,2,1)$  approximation accounted for quite a large part of  $\mathcal{R}^{(2)}$ :  $\|\mathcal{R}^{(2)}\| \approx 17.13$  and  $\|\mathcal{F}^{(2)}\| \approx 7.22$ . The  $U^{(2)} = (u_1^{(2)} \ u_2^{(2)})$  and  $w^{(2)}$  vectors are shown in Figure 5.8. Comparing  $w^{(2)}$  with the plot of  $w^{(1)}$  in Figure 5.3, we see that the second most dominating communication shown here took place essentially when the level of communication in first group was low (the angle between  $w^{(1)}$  and  $w^{(2)}$  is approximately  $86^\circ$ ).

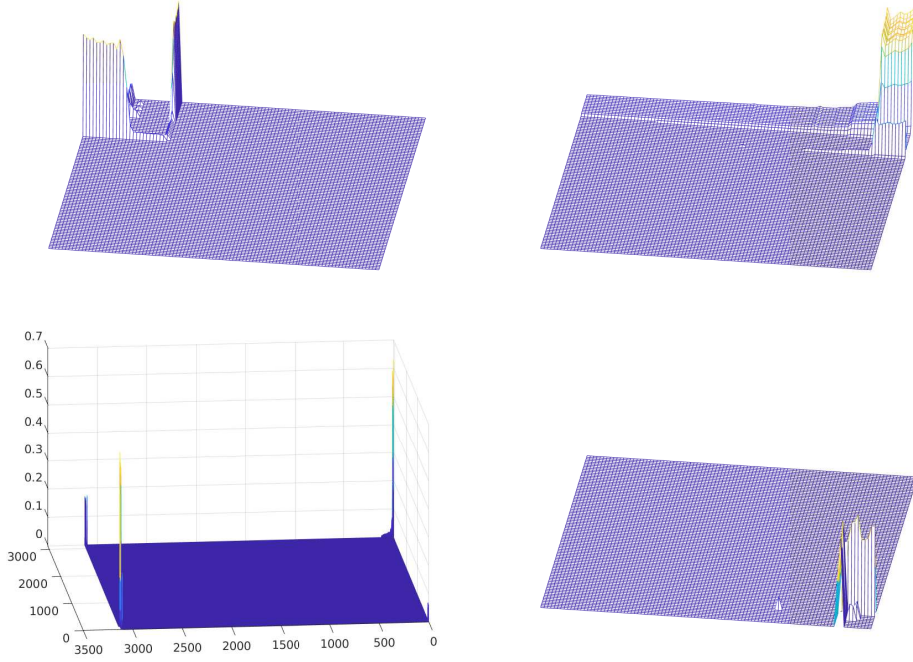


FIG. 5.5. The matrix  $\hat{B}^{(1)}$ . Top left: Close-up of the upper left corner (cf. the orientation in Figure 5.4 and in the bottom right corner). Top right: Close-up of the upper right corner. Bottom left: The whole matrix  $\hat{B}^{(1)}$  with a coarser resolution. Bottom right: Close-up of the bottom-right corner.

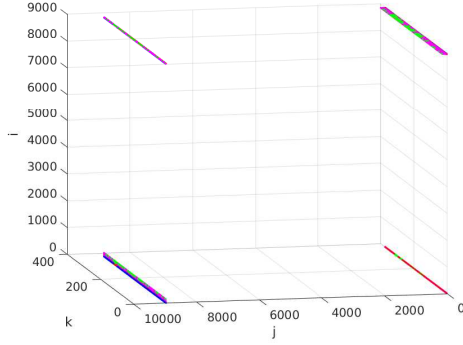


FIG. 5.6. The approximation tensor  $(w^{(1)})_3 \cdot B^{(1)}$ .

The matrix  $\hat{B}^{(2)}$  is shown in Figure 5.9. The approximation tensor  $(w^{(2)})_3 \cdot \hat{B}^{(2)}$  looked very similar to  $(w^{(1)})_3 \cdot \hat{B}^{(1)}$  in Figure 5.6.

Again we deflated the tensor, and performed another step of analysis on  $\mathcal{B}^{(3)}$ . The core tensor was

$$\begin{pmatrix} 1.82 & 0 \\ 0 & 2.06 \end{pmatrix},$$

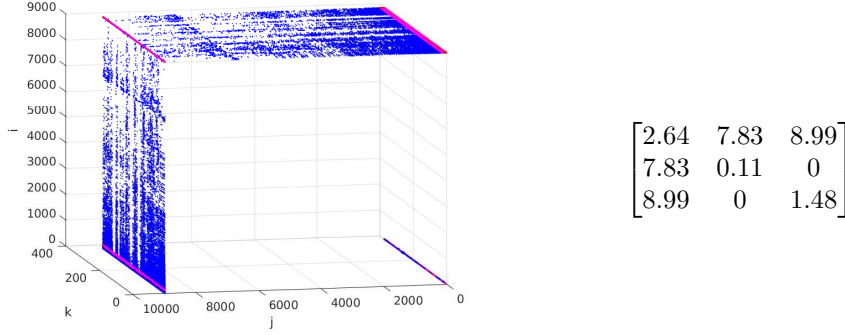


FIG. 5.7. Left: Deflated 1998DARPA tensor  $\mathcal{R}^{(2)}$ . Right: Norms of the tensor blocks

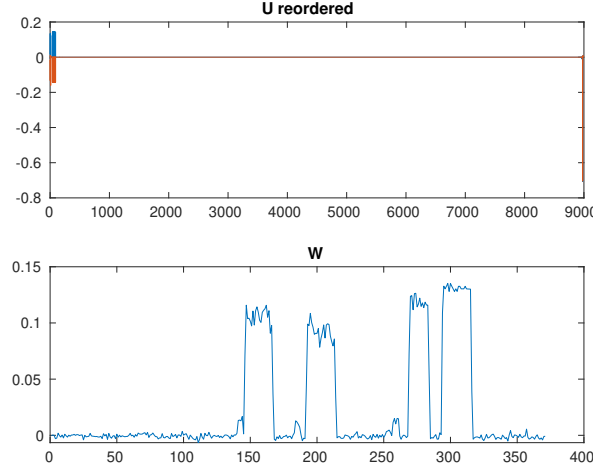


FIG. 5.8. Analysis of the deflated tensor  $\mathcal{R}^{(2)}$ . Top: the vectors  $u_1^{(2)}$  (blue),  $u_2^{(2)}$  (red). Bottom:  $w^{(2)}$ .

$\|\mathcal{R}^{(3)}\| \approx 15.54$  and  $\|\mathcal{F}^{(3)}\| \approx 2.76$ . The  $U$  and  $W$  vectors are shown in Figure 5.10. The matrix  $\hat{B}^{(3)}$  is illustrated in Figure 5.11. The approximation tensor  $(w^{(3)})_3 \cdot B^{(3)}$  looked very similar to those in the previous steps.

The procedure so far can be written in the form

$$\mathcal{A}^{(1)} \approx \sum_{\nu=1}^3 \left( w^{(\nu)} \right)_3 \cdot \hat{B}^{(\nu)},$$

where the terms are nonnegative tensors of rank- $(2, 2, 1)$ . Note that neither the vectors  $w^{(\nu)}$  nor the matrices  $\hat{B}^{(\nu)}$  are orthogonal (with Euclidean inner products). However, for this example where the tensor  $\mathcal{A}$  is sparse and nonnegative, we have computed a few terms of a *sparse, nonnegative low rank expansion*.

In the case when the 3-slices of the tensor  $\mathcal{A}$  are adjacency matrices of graphs, we can interpret the matrices  $\hat{B}^{(\nu)}$  in the expansion as adjacency matrices of dominating or *salient subgraphs*. The element  $w_k^{(\nu)} > 0$  of the vector  $w^{(\nu)}$  can be seen as a measure of how much of the salient subgraph corresponding to  $\hat{B}^{(\nu)}$  is present in the slice  $k$  of the tensor.

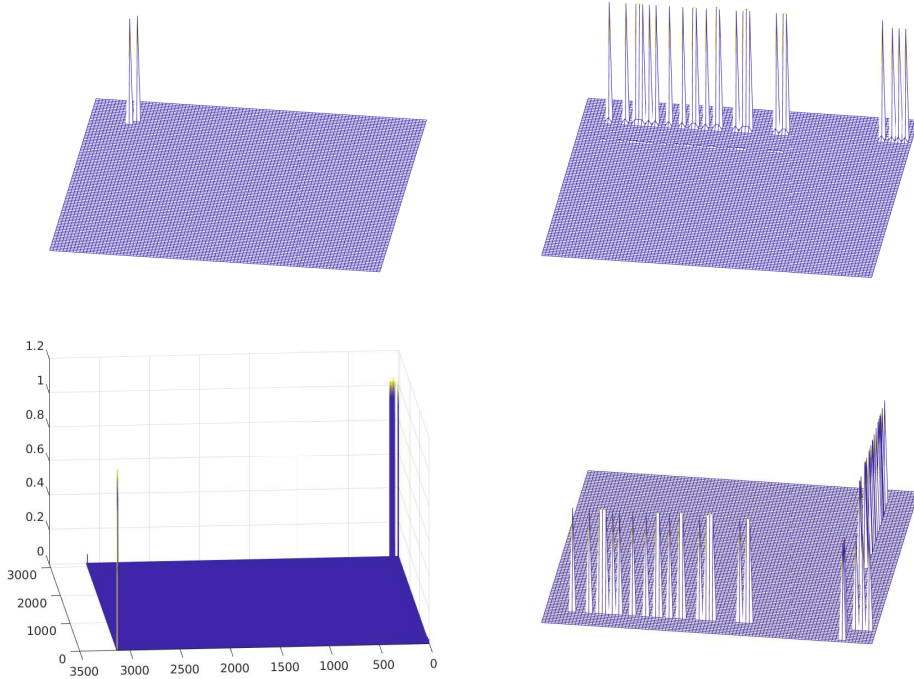


FIG. 5.9. The matrix  $\widehat{R}^{(2)}$ . Top left: Close-up of the upper left corner. Top right: Close-up of the upper right corner. Bottom left: the whole matrix with a coarser resolution. Bottom right: Close-up of the lower right corner.

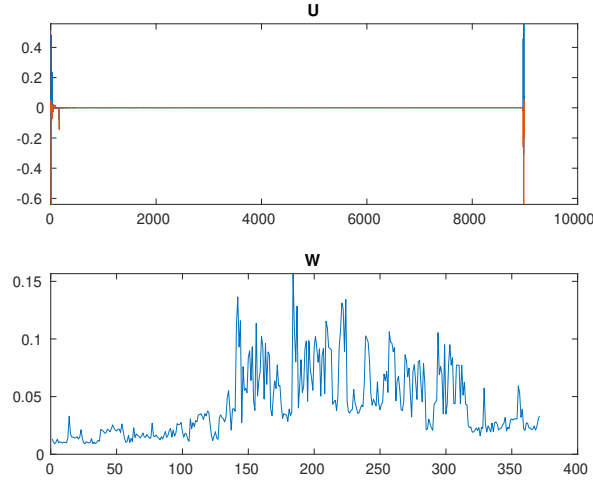


FIG. 5.10. Analysis of the deflated tensor  $\mathcal{R}^{(3)}$ . Top: the vectors  $u_1^{(3)}$  (blue),  $u_2^{(3)}$  (red). Bottom:  $w^{(3)}$ .

To check how much the different terms in the expansion overlapped, we computed

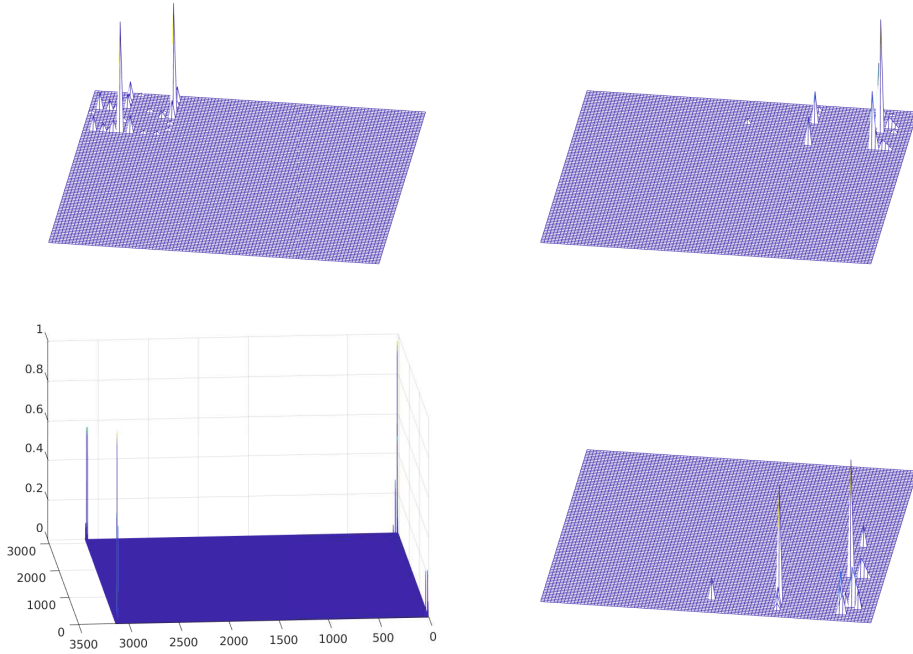


FIG. 5.11. The matrix  $\widehat{B}^{(3)}$ . Top left: Close-up of the upper left corner. Top right: Close-up of the upper right corner. Bottom left: the whole matrix with a coarser resolution. Bottom right: Close-up of the lower right corner.

the cosine of the angles between the matrices,

$$\cos(\widehat{B}^{(\nu)}, \widehat{B}^{(\lambda)}) = \frac{\langle \widehat{B}^{(\nu)}, \widehat{B}^{(\lambda)} \rangle}{\|\widehat{B}^{(\nu)}\| \|\widehat{B}^{(\lambda)}\|},$$

and give them below Table 5.1 (the cosine is a measure of overlap between edges in the communication graphs). There we also give the norms on  $\widehat{B}^{(\nu)}$  and  $\mathcal{F}^{(\nu)}$ . As the identity  $\|B^{(\nu)}\| = \|\mathcal{F}^{(\nu)}\|$  holds, it is seen that the elements in  $\mathcal{B}^{(\nu)}$  that are removed in the thresholding (5.3) are insignificant.

Summarizing the experiment, we have computed an approximate expansion of the tensor that corresponds to three relatively small and almost disjoint groups of IP addresses that dominate the communication. The communication corresponding to the first two terms in the expansion is taking place at different times.

**5.2. Low Rank Expansion of News Text.** In this section we will compute a low rank expansion of seven terms,

$$\mathcal{A} \approx \sum_{\nu=1}^7 \left( w^{(\nu)} \right)_3 \cdot \widehat{B}^{(\nu)},$$

for the Reuters news text tensor that we analyzed in Section 3. The matrices  $\widehat{B}^{(\nu)}$  are considered as adjacency matrices of subgraphs of the large graph corresponding to cooccurrence of all 13332 terms in the sentences of the texts, cf. Section 3.

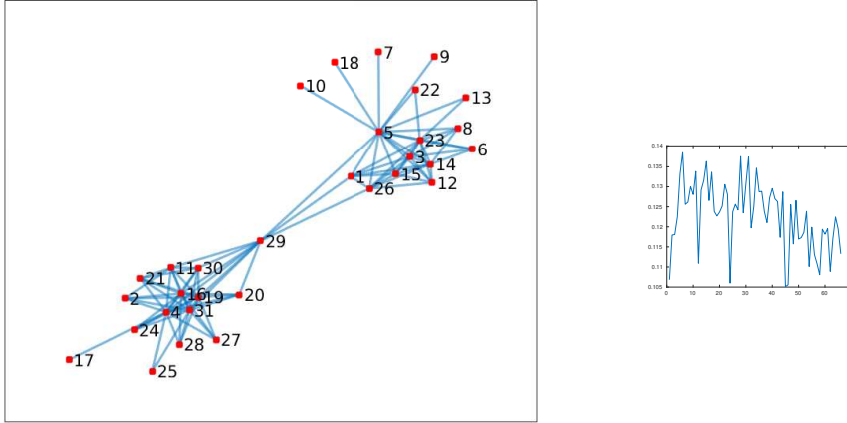
TABLE 5.1

Network Traffic example. Top: Norms of  $\hat{B}^{(\nu)}$  and  $\mathcal{F}^{(\nu)}$ , the largest and smallest values of  $B^{(\nu)}$  (i.e. before thresholding), and the eigenvalues of  $\mathcal{F}^{(\nu)}$ . Bottom: Cosines of the angles between the matrices  $\|\hat{B}^{(\nu)}\|$ ,  $C_B(\mu, \lambda) = \cos(\hat{B}^{(\nu)}, \hat{B}^{(\lambda)})$ .

$\ \hat{B}^{(\nu)}\ $	8.8	7.2	2.8
$\ \mathcal{F}^{(\nu)}\ $	8.8	7.2	2.08
max	0.63	1.0	0.97
min	-0.02	-0.07	-0.08
$\lambda_1$	6.3	5.1	2.1
$\lambda_2$	-6.1	-5.1	1.8

$$C_B = \begin{bmatrix} 1 & 0.07 & 0.06 \\ & 1 & 0.006 \\ & & 1 \end{bmatrix}.$$

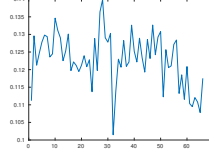
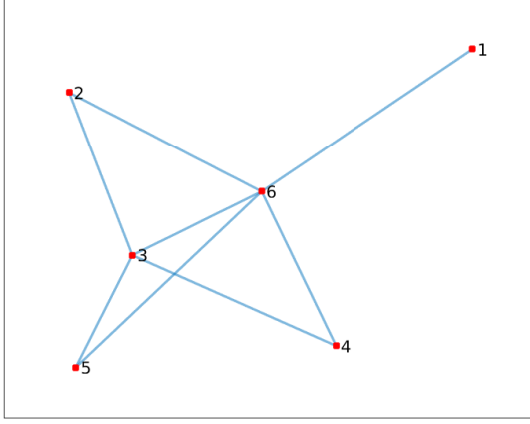
In the construction of the  $\hat{B}^{(\nu)}$  matrices we used the value  $\theta = 0.25$  for the cut-off parameter (5.3). The seven terms are illustrated in Figures 5.12–5.18.



- |                |               |                  |                |                     |
|----------------|---------------|------------------|----------------|---------------------|
| 1. afghanistan | 8. fugitive   | 15. network      | 22. rule       | 29. united_states   |
| 2. airliner    | 9. group      | 16. new_york     | 23. saudi-born | 30. washington      |
| 3. al.quaeda   | 10. guerrilla | 17. official     | 24. sept       | 31. world_trade_ctr |
| 4. attack      | 11. hijack    | 18. organization | 25. suicide    |                     |
| 5. bin_laden   | 12. islamic   | 19. pentagon     | 26. taliban    |                     |
| 6. dissident   | 13. leader    | 20. people       | 27. tower      |                     |
| 7. exile       | 14. militant  | 21. plane        | 28. twin       |                     |

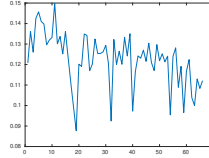
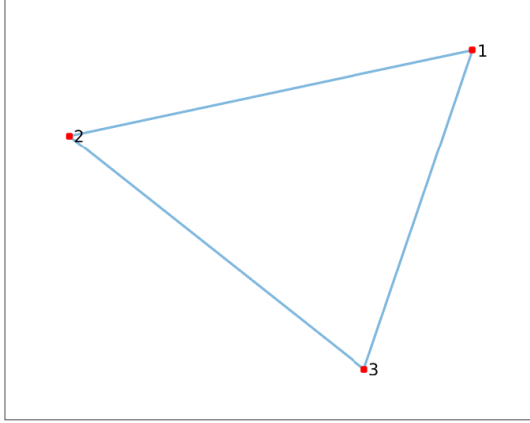
FIG. 5.12. First term in the expansion of the news text tensor. We illustrate the graph, the vector  $w^{(1)}$ , and the keywords corresponding to the vertices in the graph. Two subgraphs are visible, connected via the term “united\_states”; the two subtopics are close to  $T^1$  and  $T^2$  in Table 3.1.

In Table 5.2 we give the norms of the terms in the expansion, i.e., the norms of the matrices  $\hat{B}^{(\nu)}$ . For comparison we also give the norms of the tensors  $\mathcal{F}^{(\nu)}$ , which are equal to the norms of the terms before thresholding. It is seen that the thresholding



1. news 2. reporter 3. reuter 4. rumsfeld 5. sec 6. tell

FIG. 5.13. *Second term.*

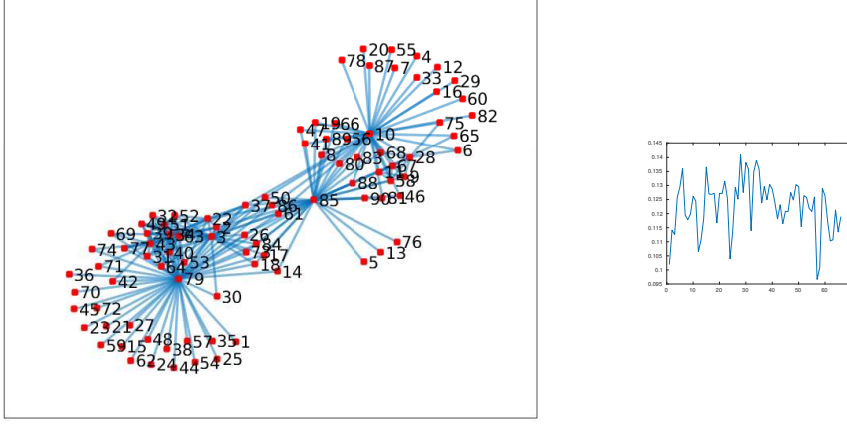


1. powell 2. rumsfeld 3. sec

FIG. 5.14. *Third term.*

removes a considerable number of elements from  $\mathcal{B}^{(\nu)}$ . Note that the terms are given approximately in descending order of magnitude. To check how much the different terms in the expansion overlapped, we computed the cosine of the angles between the matrices  $\widehat{B}^{(\nu)}$  (the cosine is a measure of overlap between edges in the graphs). There was some overlap, as seen in Table 5.2, but mostly not significant. The vectors  $w^{(i)}$ , on the other hand, are nonnegative and some of them are almost linearly dependent.

For comparison we also ran a test, where we used a threshold on the absolute values in (5.3), with  $\theta = 0.25$  as before. As expected, the subgraphs were larger (words corresponding to negative elements in the  $B^{(\nu)}$  were retained), but otherwise the expansion was quite similar.

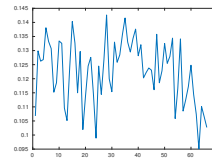
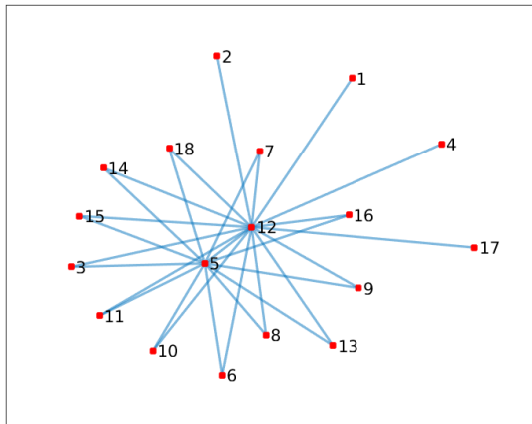


- |                      |                    |                       |                   |
|----------------------|--------------------|-----------------------|-------------------|
| 1. abdul_salam_zaeef | 25. general        | 49. northern_alliance | 73. strike        |
| 2. afghan            | 26. government     | 50. official          | 74. stronghold    |
| 3. afghanistan       | 27. group          | 51. omar              | 75. suicide       |
| 4. agent             | 28. hijack         | 52. opposition        | 76. support       |
| 5. air               | 29. hijacker       | 53. pakistan          | 77. supreme       |
| 6. airliner          | 30. islamic        | 54. pakistani         | 78. suspect       |
| 7. america           | 31. kabul          | 55. passenger         | 79. taliban       |
| 8. american          | 32. kandahar       | 56. people            | 80. terrorism     |
| 9. anthrax           | 33. law            | 57. pervez            | 81. terrorist     |
| 10. attack           | 34. leader         | 58. plane             | 82. threat        |
| 11. bin_laden        | 35. line           | 59. position          | 83. time          |
| 12. biological       | 36. mazar-i-sharif | 60. possible          | 84. troop         |
| 13. bomb             | 37. military       | 61. pres_bush         | 85. united_states |
| 14. campaign         | 38. minister       | 62. president         | 86. war           |
| 15. capital          | 39. mohammad       | 63. rule              | 87. warfare       |
| 16. case             | 40. mohammad_omar  | 64. ruler             | 88. washington    |
| 17. city             | 41. month          | 65. saudi-born        | 89. week          |
| 18. country          | 42. movement       | 66. security          | 90. world         |
| 19. day              | 43. mullah         | 67. sept              |                   |
| 20. deadly           | 44. musharraf      | 68. september         |                   |
| 21. fighter          | 45. muslim         | 69. southern          |                   |
| 22. force            | 46. new            | 70. special           |                   |
| 23. foreign          | 47. new_york       | 71. spiritual         |                   |
| 24. front            | 48. northern       | 72. spokesman         |                   |

FIG. 5.15. *Fourth term.*

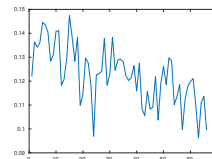
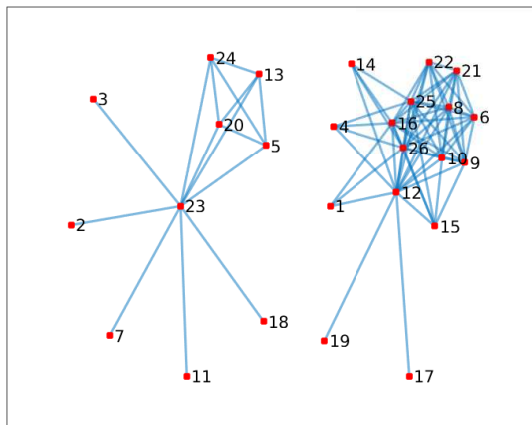
**5.3. Summary of the Algorithm and Computational Issues.** The low rank expansion algorithm is summarized below. The 3-slices of initial tensor  $\mathcal{A} = \mathcal{R}^{(1)}$  are normalized.





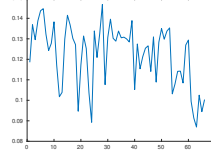
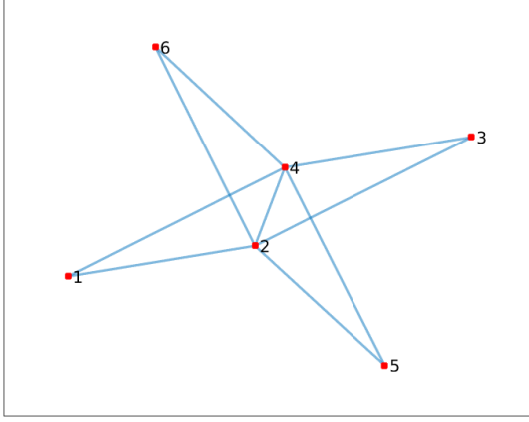
- |               |                   |              |                     |
|---------------|-------------------|--------------|---------------------|
| 1. agency     | 6. enforcement    | 11. new_york | 16. washington      |
| 2. anchor     | 7. law            | 12. news     | 17. white_house     |
| 3. brief      | 8. mayor          | 13. official | 18. world_trade_ctr |
| 4. brokaw     | 9. mayor_giuliani | 14. pentagon |                     |
| 5. conference | 10. nbc           | 15. tom      |                     |

FIG. 5.16. *Fifth term.*



- |                |                    |                  |                     |
|----------------|--------------------|------------------|---------------------|
| 1. 110-story   | 8. law             | 15. pennsylvania | 22. twin            |
| 2. afghanistan | 9. mayor           | 16. pentagon     | 23. united_states   |
| 3. attack      | 10. mayor_giuliani | 17. people       | 24. war             |
| 4. city        | 11. military       | 18. pres_bush    | 25. washington      |
| 5. conference  | 12. new_york       | 19. tell         | 26. world_trade_ctr |
| 6. enforcement | 13. news           | 20. terrorism    |                     |
| 7. force       | 14. official       | 21. tower        |                     |

FIG. 5.17. *Sixth term.*



1. agency                      3. federal    5. official  
2. enforcement    4. law                      6. united\_states

FIG. 5.18. *Seventh term.*

TABLE 5.2

*Top: Norms of  $\hat{B}^{(\nu)}$ ,  $\mathcal{F}^{(\nu)}$ , the largest and smallest values of  $B^{(\nu)}$  (i.e. before thresholding), and the eigenvalues of the  $\mathcal{F}^{(\nu)}$ . Bottom: Cosines of the angles between the matrices  $\hat{B}^{(\nu)}$ .*

$\ \hat{B}^{(\nu)}\ $	2.7	1.9	1.8	1.9	1.2	1.6	1.0
$\ \mathcal{F}^{(\nu)}\ $	6.1	5.6	5.4	5.4	5.1	5.1	5.0
max	0.46	0.84	1.0	0.24	0.43	0.27	0.54
min	-0.24	-0.11	-0.37	-0.12	-0.13	-0.25	-0.17
$\lambda_1$	5.1	4.7	4.7	4.7	4.4	4.4	4.4
$\lambda_2$	3.4	2.9	2.8	2.6	2.5	2.5	2.4

$$C = \begin{bmatrix} 1 & 0 & 0 & 0.14 & 0 & 0.21 & 0 \\ & 1 & 0 & 0 & 0 & 0 & 0 \\ & & 1 & 0 & 0 & 0 & 0 \\ & & & 1 & 0 & 0.04 & 0 \\ & & & & 1 & 0.11 & 0 \\ & & & & & 1 & 0.06 \\ & & & & & & 1 \end{bmatrix} \quad C_{\mu\lambda} = \cos(\hat{B}^{(\nu)}, \hat{B}^{(\lambda)}).$$

---

**Indata:**  $\mathcal{A} = \mathcal{R}^{(1)}$ ,  $\theta$ ,  $q$ ,    **Outdata:** Expansion  $\mathcal{A} \approx \sum_{\nu=1}^q (w^{(\nu)})_3 \cdot \hat{B}^{(\nu)}$

---

**for**  $\nu = 1 : q$

    Compute best rank-(2,2,1) approximation of  $\mathcal{R}^{(\nu)}$ ,  
         giving  $(U^{(\nu)}, U^{(\nu)}, w^{(\nu)})$ , and  $\mathcal{F}^{(\nu)}$

    Compute  $B^{(\nu)} = (U^{(\nu)}, U^{(\nu)})_{1,2} \cdot \mathcal{F}^{(\nu)}$

    Apply threshold (5.3), giving  $\hat{B}^{(\nu)}$

$\mathcal{R}^{(\nu+1)} = \mathcal{R}^{(\nu)} - (w^{(\nu)})_3 \cdot \hat{B}^{(\nu)}$     26

**end**

---

In the example in Section 5.1 the sparse tensor  $\mathcal{A}$  requires approximately 6 megabytes storage. The way we construct the matrices  $\widehat{B}^{(\nu)}$  they are very sparse: between 4 and 77 kilobytes storage. The deflation producing  $\mathcal{R}^{(2)}, \mathcal{R}^{(3)}, \dots$  incurs some fill-in so that, e.g.,  $\mathcal{R}^{(3)}$  requires 56 megabytes. However, it is not necessary to perform the deflation explicitly. In the Krylov-Schur method only the action of the tensor on narrow blocks of vectors is required. Therefore one can keep the deflated tensor in the form of the original tensor minus the low rank terms, e.g.,

$$\mathcal{R}^{(3)} = \mathcal{A} - \sum_{\nu=1}^2 \left( w^{(\nu)} \right)_3 \cdot \widehat{B}^{(\nu)}.$$

The action of  $\mathcal{B}^{(3)}$  on a block of vectors is then only marginally more expensive than the action of  $\mathcal{R}^{(1)}$ .

**6. Conclusions.** In several applications there is a need to analyze data organized in tensors. The aim of this paper has been to show that the best rank-(2,2,2) and rank-(2,2,1) approximations can be used to extract useful information from large and sparse 3-tensors from a few applications. The methods can be considered as generalizations of spectral graph partitioning.

In the first text analysis example the tensor was (1,2)-symmetric, and consisted of a sequence of cooccurrence graphs for terms in news text. The aim was to find the main topics. The tensor method detected structure that was not visible when a corresponding spectral matrix method was used (probably because in the latter the abundance of insignificant terms obscured the relevant information).

In the second example the tensor was non-symmetric, and represented authors and terms at conferences over 17 years. We demonstrated that the tensor spectral method could simultaneously reveal structure in all three modes.

We then presented an algorithm for computing a rank-(2,2,1) expansion of a (1,2)-symmetric tensor. It was applied to analyze a tensor that represented network traffic logs. The dominating communication was found, and it was shown that a small number of users accounted for most of the communication. It was shown that the tensor was much sparser than could be seen initially. In the second text analysis example we used the same news texts as in the first. The rank-(2,2,1) expansion found dominating subgraphs.

In this paper it has not been our intention to give a comprehensive treatment of the use of best rank-(2,2,1) and rank-(2,2,2) approximations to tensor data from applications. Instead, we have demonstrated a few problems with real data, where our methods were able to find relevant structure. These examples show that the proposed methods are potentially powerful tools for the analysis of large and sparse data with tensor structure. Further investigations into the use of our methods are needed.

## REFERENCES

- [1] P.-A. Absil, R. Mahony, and R. Sepulchre. *Optimization Algorithms on Matrix Manifolds*. Princeton University Press, 2007.
- [2] P.A. Absil, R. Mahoney, R. Sepulchre, and P. Van Dooren. A Grassman-Rayleigh quotient iteration for computing invariant subspaces. *SIAM Review*, 44:57–73, 2002.
- [3] V. Batagelj and A. Mrvar. Density based approaches to network analysis. Analysis of Reuters terror news network. In *Ninth Annual ACM SIGKDD, Washington, D.C.*, 2003.
- [4] X. Cao, X. Wei, Y. Han, Y. Yang, and D. Lin. Robust Tensor Clustering with Non-Greedy Maximization. In *IJCAI’13 Proceedings of the Twenty-Third International Joint Conference on Artificial Intelligence*, pages 1254–1259, 2013.

- [5] Y. Chen, X. Xiao, and Y. Zhou. Multi-view subspace clustering via simultaneously learning the representation tensor and affinity matrix. *Pattern Recognition*, 106:107441, 2020.
- [6] F. Chung. *Spectral Graph Theory*. CBMS Regional Conference Series in Mathematics Number 92. American Mathematical Society, 1997.
- [7] L. De Lathauwer, B. De Moor, and J. Vandewalle. A Multilinear Singular Value Decomposition. *SIAM J. Matrix Anal. Appl.*, 21:1253–1278, 2000.
- [8] L. De Lathauwer, B. De Moor, and J. Vandewalle. On the Best Rank-1 and Rank- $(R_1, R_2, \dots, R_N)$  Approximation of Higher-Order Tensor. *SIAM J. Matrix Anal. Appl.*, 21:1324–1342, 2000.
- [9] V. de Silva and L.-H. Lim. Tensor Rank and the Ill-Posedness of the Best Low-Rank Approximation Problem. *SIAM Journal on Matrix Analysis and Applications*, 30(3):1084–1127, 2008.
- [10] I. S. Dhillon. Co-Clustering Documents and Words Using Bipartite Spectral Graph Partitioning. In *Proc. 7th ACM-SIGKDD Conference*, pages 269–274, 2001.
- [11] A. Edelman, T. Arias, and S. T. Smith. The Geometry of Algorithms with Orthogonality Constraints. *SIAM J. Matrix Anal. Appl.*, 20:303–353, 1998.
- [12] L. Eldén. *Matrix Methods in Data Mining and Pattern Recognition, Second Edition*. SIAM, 2019.
- [13] L. Eldén and M. Dehghan. A Krylov-Schur like method for computing the best rank- $(r_1, r_2, r_3)$  approximation of large and sparse tensors. to appear, 2020.
- [14] L. Eldén and M. Dehghan. Spectral partitioning of large and sparse tensors using low-rank tensor approximation. to appear, 2020.
- [15] L. Eldén and B. Savas. A Newton-Grassmann method for computing the Best Multi-Linear Rank- $(r_1, r_2, r_3)$  Approximation of a Tensor. *SIAM J. Matrix Anal. Appl.*, 31:248–271, 2009.
- [16] L. Eldén and B. Savas. Perturbation Theory and Optimality Conditions for the Best Multilinear Rank Approximation of a Tensor. *SIAM J. Matrix Anal. Appl.*, 32:1422–1450, 2011.
- [17] A. Globerson, G. Chechik, F. Pereira, and N. Tishby. Euclidean Embedding of Co-occurrence Data. *The Journal of Machine Learning Research*, 8:2265–2295, 2007.
- [18] G. H. Golub and C. F. Van Loan. *Matrix Computations. 4th ed*. SIAM, 2013.
- [19] F. L. Hitchcock. Multiple Invariants and generalized rank of a p-way matrix or tensor. *J. Math. Phys. Camb.*, 7:39–70, 1927.
- [20] M. Ishteva, L. De Lathauwer, P.-A. Absil, and S. Van Huffel. Differential-geometric Newton method for the best rank- $(R_1, R_2, R_3)$  approximation of tensors. *Numer. Algor.*, 51:179–194, 2008. Published online 22 Nov 2008.
- [21] Mariya Ishteva, P.-A. Absil, Sabine Van Huffel, and Lieven De Lathauwer. Best Low Multilinear Rank Approximation of Higher-Order Tensors, Based on the Riemannian Trust-Region Scheme. *SIAM Journal on Matrix Analysis and Applications*, 32(1):115–135, 2011.
- [22] S. Jegelka, Sra S., and A. Banerjee. Approximation Algorithms for Tensor Clustering. In *The 20th International Conference on Algorithmic Learning Theory (ALT)*, 2009.
- [23] I. Jeon, E. Papalexakis, C. Faloutsos, L. Sael, and U. Kang. Mining Billion-Scale Tensors: Algorithms and Discoveries. *The VLDB Journal*, 25(4):519–544, August 2016.
- [24] R. Lehoucq, D. Sorensen, and C. Yang. *Arpack Users’ Guide: Solution of Large Scale Eigenvalue Problems with Implicitly Restarted Arnoldi Methods*. SIAM, Philadelphia, 1998.
- [25] X. Liu, L. De Lathauwer, F. Janssens, and B. De Moor. Hybrid Clustering of Multiple Information Sources via HOSVD. In L. Zhang, B.-L. Lu, and J. Kwok, editors, *Advances in Neural Networks - ISNN 2010*, volume 6064 of *Lecture Notes in Computer Science*, pages 337–345. Springer Berlin Heidelberg, 2010.
- [26] A. Pothen, H. D. Simon, and K.-P. Liou. Partitioning Sparse Matrices with Eigenvectors of Graphs. *SIAM Journal on Matrix Analysis and Applications*, 11(3):430–452, 1990.
- [27] M. A. Riolo and M. E. J. Newman. First-principles multiway spectral partitioning of graphs. *Journal of Complex Networks*, 2014.
- [28] B. Savas and L.-H. Lim. Quasi-Newton Methods on Grassmannians and Multilinear Approximations of Tensors. *SIAM Journal on Scientific Computing*, 32(6):3352–3393, 2010.
- [29] S. Smith, J. W. Choi, J. Li, R. Vuduc, J. Park, X. Liu, and G. Karypis. FROSTT: The Formidable Repository of Open Sparse Tensors and Tools, 2017.
- [30] U. von Luxburg. A tutorial on spectral clustering. *Statistics and Computing*, 17:395–416, 2007.
- [31] Z. Wei, H. Zhao, L. Zhao, and H. Yan. Multiscale co-clustering for tensor data based on canonical polyadic decomposition and slice-wise factorization. *Information Sciences*, 503:72 – 91, 2019.
- [32] H. Xu, X. Zhang, W. Xia, Q. Gao, and X. Gao. Low-rank tensor constrained co-regularized multi-view spectral clustering. *Neural Networks*, 132:245 – 252, 2020.

- [33] W. W. Zachary. An Information Flow Model for Conflict and Fission in Small Groups. *Journal of Anthropological Research*, 33:452–473, 1977.
- [34] T. Zhang and G. H. Golub. Rank-One Approximation to Higher Order Tensors. *SIAM J. Matrix Anal. Appl.*, 23:534–550, 2002.